IEEE Access
Multidisciplinary | Rapid Review | Open Access Journal

Received September 1, 2020, accepted September 6, 2020, date of publication September 9, 2020,
date of current version September 23, 2020.

Digital Object Identifier 10.1109/ACCESS.2020.3022881

Autonomous Quadcopter Precision Landing Onto a Heaving Platform: New Method and Experiment

NGUYEN XUAN-MUNG[1], (Member, IEEE), SUNG KYUNG HONG[1], NGOC PHI NGUYEN[1], LE NHU NGOC THANH HA[2], AND TIEN-LOC LE[1], (Member, IEEE)

[1]Faculty of Mechanical and Aerospace Engineering, Sejong University, Seoul 05006, South Korea
[2]Faculty of Intelligent Mechatronics Engineering, Sejong University, Seoul 05006, South Korea

Corresponding author: Sung Kyung Hong (skhong@sejong.ac.kr)

This work was supported by the Ministry of Science and ICT (MSIT), South Korea, under the Information Technology Research Center (ITRC) support program (IITP-2020-2018-0-01423) supervised by the Institute for Information and Communications Technology Promotion (IITP); and by Basic Science Research Program through the National Research Foundation of Korea (NRF) funded by the Ministry of Education (2020R1A6A1A03038540).

ABSTRACT Nowadays, with the increasing popularity of quadcopter unmanned aerial vehicles in several real-world applications, achieving a fully autonomous quadcopter flight has become an imperative topic investigated in many studies. One of the most pressing issues in such a topic is the precision landing task, which always is devastatingly influenced by the ground effect and external disturbances. In this paper, we present an autonomous quadcopter landing algorithm allowing the vehicle to land robustly and precisely onto a heaving platform. Firstly, a robust control algorithm addressing the altitude flight under the ground effect and external disturbances is derived. We strictly prove the closed-loop system stability by using the Lyapunov theory. Secondly, a landing target state estimator is proposed to provide state estimations of the moving landing target. In addition, we propose a landing procedure to ensure the landing task is achieved safely and reliably. Finally, we use a DJI-F450 drone equipped with an infrared sensor and a laser ranging sensor as the experimental quadcopter platform and conduct experiments to evaluate the performance of our new algorithm in real flight conditions. The experimental results demonstrate the effectiveness of the proposed method.

INDEX TERMS Autonomous landing, precision landing, moving target, quadcopter, heaving platform, ship deck, robust control, sliding mode control, disturbance observer.

I. INTRODUCTION

Unmanned aerial vehicles (UAVs) are playing essential roles in a variety of today's applications in several areas such as civil engineering, military applications, scientific research. Specific applications to be listed include delivery services, aerial mapping, search and rescue operations, surveillance, and risk zone inspections [1]. An important class of UAVs is quadcopters that have attracted great attention from researchers due to their superior properties such as high maneuverability, reliability, diverse applicability, and economy [2]. However, the quadcopter, which has to perform six-degrees-of-freedom flight with only four control inputs [3], is known as a typical example of a coupled underactuated system. Additionally, the ground effect and external disturbances can further complicate the design of controllers for the quadcopter. In order to deal with the control problem of such systems, a number of control algorithms were studied, such as a proportional-integral-derivative (PID) controller in [4], backstepping method in [5], a robust sliding mode controller (SMC) in [6], a second-order SMC subject to a known mismatched term in [7], a disturbance-observer-based robust algorithm coping with unpredictable time-varying disturbances in [8], and a resilient approach in [9]. Although many control techniques were investigated, designing high-performance controllers for quadcopters remains challenging and is widely undertaken in the scientific community.

The limited payload of a quadcopter limits the battery amount it can carry. Hence, the vehicle needs to land frequently for battery replacing or recharging after short periods of operation. Besides, the landing task is one of the primary missions the quadcopter has to exhibit in applications such as delivery services, environment exploration, surveillance. These facts make the quadcopter's autonomous landing problem an imperative topic. An optical-flow-based strategy is

The associate editor coordinating the review of this manuscript and approving it for publication was Shihong Ding.

proposed in [10] to achieve the landing task of a micro air vehicle by adjusting the controller gains. In [11], another approach is presented for a quadcopter based on the velocity vector field method. While these studies only considered fixing the landing pads on flat platforms, the authors of [12] addressed a robust controller allowing a quadcopter to land on a slope. In another study on landing onto such a steep platform presented in [13], the authors introduced a landing method by estimating the ground orientation using a camera.

Although attracting a certain number of studies, the algorithms for landing on fixed platforms cannot satisfy landing performance requirements when the platforms are set in motion. Therefore, the problem of landing onto mobile targets has been investigated. The authors of [14] proposed a vision-based solution for the problem of quadcopter landing onto a heaving (vertically moving) platform. Since this study makes use of a motion capture system, it is not applicable for outdoor applications. In another research presented in [15], the authors used the global positioning system (GPS) navigation to enable a quadcopter to find a moving platform and a vision-based control to approach and land onto it. Many other vision-based approaches coming with different controllers were presented including the studies in [16] with a model predictive controller, [17] with adaptive proportional-integral-derivative (PID) altitude controllers, [18] with a neural network controller, [19] with a multi-level fuzzy logic controller, and [20] with a backstepping controller. Meanwhile, some other approaches focus more on improving the landing target state estimation [21]–[24]. As described in [22], a gimbaled camera is used to make sure the landing target is detected when the vehicle is getting close to the moving platform. In [24], an adequate landing pad composed of different-sized patterns is designed, allowing the camera to detect them from high as well as low altitudes.

Compared with other mobile landing platforms, a ship deck environment makes the landing task more challenging due to the influences of the sea waves and strong disturbances such as the wind. Dealing with such an issue, the authors of [25]–[28] proposed different methods using different control techniques, including PID [25], sliding mode control [26], robust linear feedback control [27]. However, these studies only stopped at verifying the proposed algorithm through numerical simulations. Going one step further, the approaches [29] and [30] presented vision-based vessel deck algorithms and experimentally demonstrated the proposed methods using real quadcopters and ship deck emulators. However, the vertical strokes of these emulators are only a few centimeters that are not enough to simulate the heaving motion of a real vessel deck.

Most of the aforementioned studies are somehow vision-based approaches that limit their applicability during the night time and/or in light-lacking environments. Furthermore, among them, only a few approaches address the problem of landing onto a heaving platform such as a ship deck. Meanwhile, the presence of the ground effect and external disturbances, which are known as the major factors degrading the low-altitude flight performance of quadcopters [31], [32], need to be more thoroughly considered in the design of a quadcopter precision landing control. Motivated by the above observations, in this paper, we propose a synthesis algorithm allowing a quadcopter to land precisely onto a heaving platform under the influences of the ground effect and external disturbances. Our solution advances the current state-of-the-art in four ways:

(i) The infrared (IR) camera and IR beacon we use for the purpose of landing target state determination have several advantages in comparison with typical vision systems, i.e., (1) it enables the camera to detect the target even during night time and/or in light-inconvenient (too-strong or lacking) environments; and (2) the camera can detect any object that is equipped with IR LEDs, which contributes to its economical and straightforward applicability.

(ii) We derive a landing target state estimator with explicit expressions representing the position of the target in the camera-fixed, the vehicle-body-fixed, and the local earth-fixed coordinates. Using a Kalman filter, the estimator can provide stable and reliable information about the relative position and velocity between the vehicle and the landing target. This contributes to enhancing the accuracy of the precision landing task. Besides, we introduce an autonomous precision landing planner which plays the role of ensuring the landing task to be achieved safely and precisely.

(iii) A robust controller based on a disturbance observer is devised to achieve the high-performance landing task under the influences of ground effect and external disturbances. The system's stability is strictly proved by using the Lyapunov theory.

(iv) Unlike many previous studies, in which landing algorithms were only verified through numerical simulations, we conducted experimental demonstrations to highlight the effectiveness of the proposed method. Furthermore, a tough experimental scenario is carried out with the landing target placed on a heaving landing platform which simulates the vertical movement of a ship deck.

The rest of this paper is organized as follows. Section II presents the quadcopter dynamics model and problem formulation. Section III contains the main results of our work, including the design and stability analysis of the proposed robust altitude controller, the landing target state estimator, and the autonomous precision landing planner. Experimental setups, results, and discussions are given in Section IV before ending with conclusions in Section V.

II. QUADCOPTER DYNAMICS MODEL AND PROBLEM FORMULATION

In this section, we briefly present the quadcopter dynamics model as it was clearly introduced and verified in many previous studies [30], [33], [34].

Figure 1 illustrates the quadcopter configuration. The four rotors of it generate four thrust forces $F_i (i = 1, \ldots, 4)$ that

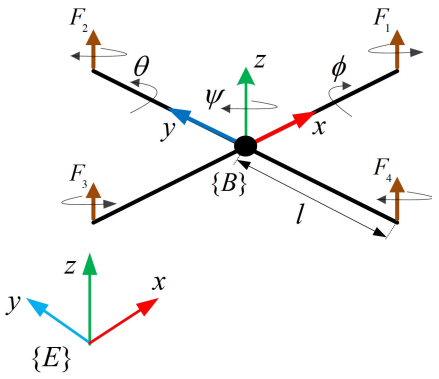

FIGURE 1. Quadcopter configuration.

have a relationship with the control inputs as:

$$\begin{cases} u_1 = F_1 + F_2 + F_3 + F_4 \\ u_2 = l(F_2 - F_4) \\ u_3 = l(F_3 - F_1) \\ u_4 = c_{fm}(-F_1 + F_2 - F_3 + F_4) \end{cases} \tag{1}$$

The full cascaded dynamics model of the vehicle is described as:

$$\begin{cases} \ddot{\phi} = \frac{I_y - I_z}{I_x}\dot{\theta}\dot{\psi} + \frac{l}{I_x}u_2 \\ \ddot{\theta} = \frac{I_z - I_x}{I_y}\dot{\phi}\dot{\psi} + \frac{l}{I_y}u_3 \\ \ddot{\psi} = \frac{I_x - I_y}{I_z}\dot{\phi}\dot{\theta} + \frac{l}{I_z}u_4 \\ \ddot{x} = \frac{1}{m}(cos\phi sin\theta cos\psi + sin\phi sin\psi)u_1 \\ \ddot{y} = \frac{1}{m}(cos\phi sin\theta sin\psi - sin\phi cos\psi)u_1 \\ \ddot{z} = -g + \frac{1}{m}(cos\phi cos\theta)u_1 \end{cases} \tag{2}$$

where x, y, z denote the position and ϕ, θ, ψ the attitude of the quadcopter in the inertial frame $\{E\}$. $m \in \mathbb{R}^+$ the mass. g the gravitational acceleration. I_x, I_y, and I_z the inertia momentum about the x, y, and z axes. l the vehicle's arm length, and c_{fm} the force-to-moment coefficient.

In order for the landing control algorithm we will present in the following section to take the ground effect and external disturbance into account, the vertical translational dynamics is rewritten with the presences of those terms as:

$$\ddot{z} = -g + \frac{\sigma}{m}(cos\phi cos\theta)u_1 + d \tag{3}$$

where

$$\sigma = \frac{1}{1 - \rho R^2(4z_r)^2} \tag{4}$$

with ρ being a positive coefficient, R the propeller radius, and z_r the vertical distance from the propeller surface to ground; and d is the external disturbance, which is assumed as being bounded and slow time-varying.

Since the value of ρ is difficult to be estimated accurately, we can only use its nominal value, $\bar{\rho}$. Let $\bar{\sigma}$ be the nominal value of σ corresponding to $\bar{\rho}$, and $\Delta\sigma$ represent the discrimination between $\bar{\sigma}$ and σ, i.e., $\Delta\sigma = \sigma - \bar{\sigma}$. Then, (3) becomes:

$$\ddot{z} = -g + \frac{\bar{\sigma} + \Delta\sigma}{m}(cos\phi cos\theta)u_1 + d \tag{5}$$

Let $D = d + \frac{cos\phi cos\theta}{m}\Delta\sigma u_1$ be the compound disturbance. Thus, (3) can be rewritten as:

$$\ddot{z} = -g + \frac{\bar{\sigma}}{m}(cos\phi cos\theta)u_1 + D \tag{6}$$

Now, the control goal is to design a robust controller u_1 to steer the quadcopter to land onto a platform that is in a heaving motion, i.e., the landing point altitude (z_d) is time-varying, despite the presences of both the system parameter uncertainty and external disturbance.

III. MAIN RESULTS

A. ROBUST ALTITUDE CONTROL ALGORITHM

In this section, a disturbance-observer-based sliding mode controller is presented for addressing the robust altitude tracking control problem of quadcopters under the presence of the compound disturbance.

Let us define the altitude tracking error as:

$$e_z = z_d - z \tag{7}$$

Thus, the derivative of e_z is:

$$\dot{e}_z = \dot{z}_d - \dot{z} \tag{8}$$

A sliding surface is introduced as:

$$s = \dot{e}_z + k_1 e_z \tag{9}$$

where $k_1 \in \mathbb{R}^+$ is a controller gain to be chosen. Then, the derivative of s is:

$$\dot{s} = \ddot{e}_z + k_1\dot{e}_z \tag{10}$$

From (8) and (10), the derivative of s can be rewritten as:

$$\dot{s} = \ddot{z}_d - \ddot{z} + k_1\dot{e}_z \tag{11}$$

To deal with the compound disturbance term, a disturbance observer is devised as follows:

$$\begin{cases} \dot{\xi} = -\lambda\xi - \lambda(\lambda\dot{z} - g + \frac{\bar{\sigma}}{m}(cos\phi cos\theta)u_1) \\ \hat{D} = \xi + \lambda\dot{z} \end{cases} \tag{12}$$

where, $\hat{D}$ is the estimate of D, λ and ξ are a positive observer gain and an auxiliary state of the observer, respectively.

Theorem 1: For a given time-varying altitude command z_d, the quadcopter system (2) with the vertical dynamics under the compound disturbance as described in (6) is ultimately stable if the followings hold:

1) the controller u_1 is designed as:

$$u_1 = \frac{m}{\bar{\sigma}cos\phi cos\theta}(\ddot{z}_d + g + k_1\dot{e}_z + k_2 s - \hat{D}) \tag{13}$$

with $\hat{D}$ being computed as in (12)

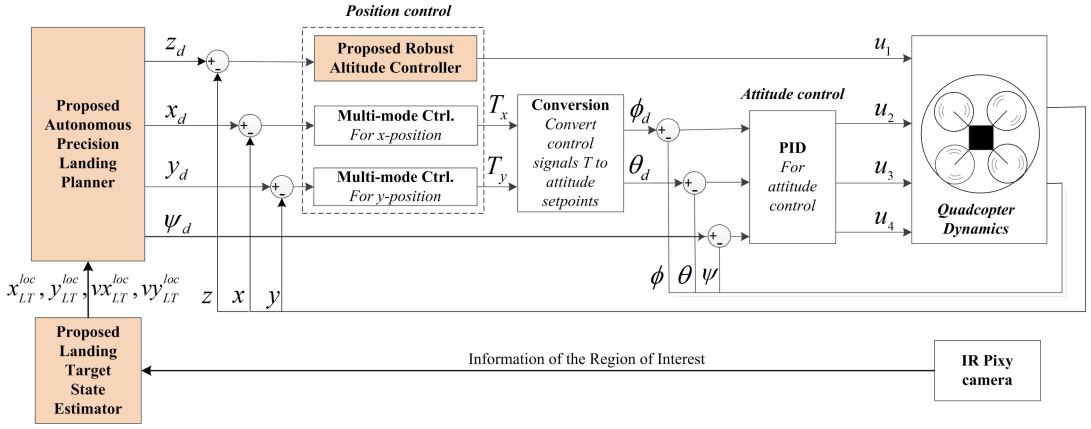

FIGURE 2. Overall block diagram of the proposed precision landing algorithm.

2) the controller and observer gains satisfy:

$$\begin{cases} k_1, & > 0 \\ k_2, & > \frac{1}{2} \\ \lambda, & > \frac{1}{2} \end{cases} \tag{14}$$

Proof: Let $\tilde{D} = D - \hat{D}$. Thus, we have

$$\begin{aligned} \dot{\tilde{D}} &= \dot{D} - \dot{\hat{\xi}} - \lambda\ddot{z} \\ &= \dot{D} + \lambda\xi + \lambda[\lambda\dot{z} - g + \frac{\bar{\sigma}}{m}(cos\phi cos\theta)u_1] - \lambda\ddot{z} \\ &= \dot{D} - \lambda\tilde{D} \end{aligned} \tag{15}$$

Choose a Lyapunov function candidate as:

$$V = \frac{1}{2}s^2 + \frac{1}{2}\tilde{D}^2 \tag{16}$$

Then, with (14), we have:

$$\begin{aligned} \dot{V} &= \dot{s}s + \dot{\tilde{D}}\tilde{D} \\ &= s[\ddot{z}_d + g - \frac{\bar{\sigma}}{m}(cos\phi cos\theta)\frac{m}{\bar{\sigma}cos\phi cos\theta}(\ddot{z}_d + g + k_1\dot{e}_z \\ &\quad + k_2 s - \hat{D}) - D + k_1\dot{e}_z] + \tilde{D}(\dot{D} - \lambda\tilde{D}) \\ &= -k_2 s^2 - \lambda\tilde{D}^2 - s\tilde{D} + \dot{D}\tilde{D} \\ &\leq -k_2 s^2 - \lambda\tilde{D}^2 + \frac{1}{2}s^2 + \frac{1}{2}\tilde{D}^2 + \frac{1}{2}\dot{D}^2 \\ &\leq -(k_2 - \frac{1}{2})s^2 - (\lambda - \frac{1}{2})\tilde{D}^2 + \epsilon \\ &\leq -2\alpha V + \epsilon \end{aligned} \tag{17}$$

where, $\alpha = min\{k_2 - \frac{1}{2}, \lambda - \frac{1}{2}\}$ and $\epsilon = \frac{1}{2}\dot{D}^2$.

From (17) and the comparison principle in [36], it is clear that the sliding surface and disturbance estimate error are ultimately bounded and, hence, the system is ultimately stable.

B. LANDING TARGET STATE ESTIMATOR

In this subsection, we derive a landing target state estimator (LTSE) which will play the role of providing information about the position and velocity of the target.

Through geometrical optics analyses (Figure 3), we introduce a way to determine the raw position information (x_{LT}^{veh} and y_{LT}^{veh}) of the landing target (LT) in the vehicle body-fixed frame $\{B\}$. This information can be obtained from the position of the LT in the camera-sensor-fixed frame $\{C\}$. Firstly, let us take a look at the similar triangles MHB and A^*CB. We have:

$$\frac{\overline{HM}}{HB} = \frac{\overline{CM^*}}{CB} \tag{18}$$

Looking at another similar triangle pair, AHB and A^*CB, we can obtain:

$$\tan\alpha_x = \frac{CA^*}{CB} \tag{19}$$

Noting that α_x and α_y are the horizontal and vertical fields of view of the camera. Substituting (19) into (18) yields:

$$\overline{HM} = \frac{HB\tan\alpha_x}{CA^*}\overline{CM^*} \tag{20}$$

With $y_{LT}^{veh} = \overline{HM}$, $z = HB$, $x_{max}^{cam} = CA^*$, and $x_{LT}^{cam} = \overline{CM^*}$, (20) can be rewritten as:

$$y_{LT}^{veh} = \frac{z\tan\alpha_x}{160}x_{LT}^{cam} \tag{21}$$

It is similar to obtain the following formula:

$$x_{LT}^{veh} = -\frac{z\tan\alpha_y}{100}y_{LT}^{cam} \tag{22}$$

After the raw position of the LT in $\{B\}$ is determined (as in (21) and (22)), a Kalman filter [37] is applied to estimate the target velocity. To that end, we move on establishing the system and measurement models of the filter.

Let $x_{LT|t}^{veh}$, $vx_{LT|t}^{veh}$, $y_{LT|t}^{veh}$, and $vy_{LT|t}^{veh}$ represent the state (including position and velocity) of the target at the time point t. Then, the state at the time point $t+1$ can be computed as:

$$\begin{bmatrix} x_{LT|t+1}^{veh} \\ vx_{LT|t+1}^{veh} \\ y_{LT|t+1}^{veh} \\ vy_{LT|t+1}^{veh} \end{bmatrix} = \begin{bmatrix} 1 & \Delta t & 0 & 0 \\ 0 & 1 & 0 & 0 \\ 0 & 0 & 1 & \Delta t \\ 0 & 0 & 0 & 1 \end{bmatrix} \begin{bmatrix} x_{LT|t}^{veh} \\ vx_{LT|t}^{veh} \\ y_{LT|t}^{veh} \\ vy_{LT|t}^{veh} \end{bmatrix} + \begin{bmatrix} 0 \\ w_{x|t} \\ 0 \\ w_{y|t} \end{bmatrix} \tag{23}$$

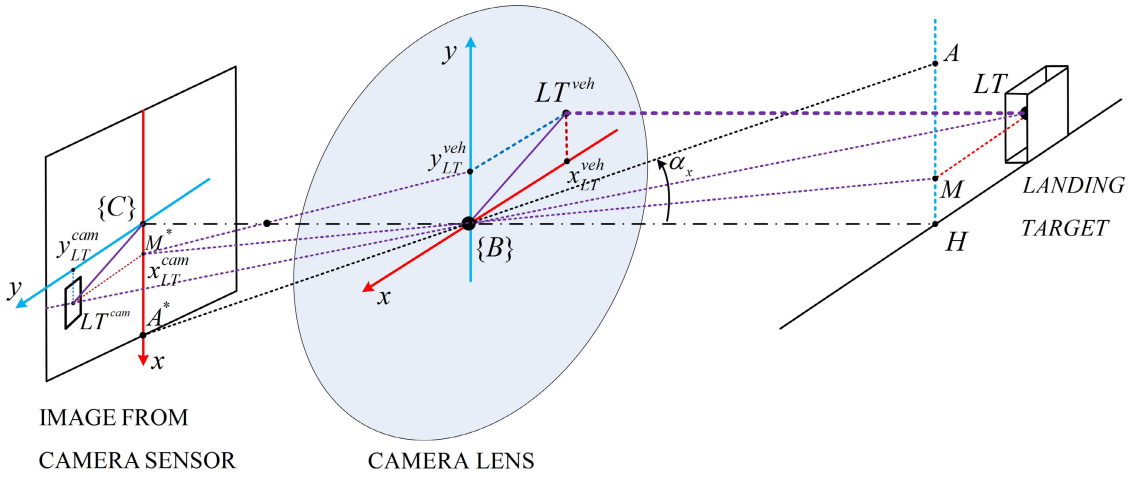

FIGURE 3. The position of the LT image in the camera-sensor-fixed frame ({*C*}) and the position of the target in the vehicle-body-fixed frame ({*B*}).

where Δt denotes the interval time measuring the position, w_x and w_y are the state transition noises. The measurement can be modeled as:

$$z_{|t} = \begin{bmatrix} 1 & 0 & 0 & 0 \\ 0 & 0 & 1 & 0 \end{bmatrix} \begin{bmatrix} x^{veh}_{LT|t} \\ vx^{veh}_{LT|t} \\ y^{veh}_{LT|t} \\ vy^{veh}_{LT|t} \end{bmatrix} + \begin{bmatrix} \upsilon_{x|t} \\ \upsilon_{y|t} \end{bmatrix} \quad (24)$$

with υ_x and υ_y being the measurement noises.

Since the quadcopter state variables used for its controllers are in $\{E\}$, the landing target state in $\{B\}$ is converted to one in $\{E\}$ (see Figure 4) by the following coordinate transformation formula:

$$\begin{bmatrix} x^{loc}_{LT} \\ vx^{loc}_{LT} \\ y^{loc}_{LT} \\ vy^{loc}_{LT} \end{bmatrix} = \begin{bmatrix} \sin\psi & 0 & -\cos\psi & 0 \\ 0 & \sin\psi & 0 & -\cos\psi \\ \cos\psi & 0 & \sin\psi & 0 \\ 0 & \cos\psi 0 & 0 & \sin\psi \end{bmatrix} \begin{bmatrix} x^{veh}_{LT} \\ vx^{veh}_{LT} \\ y^{veh}_{LT} \\ vy^{veh}_{LT} \end{bmatrix} + \begin{bmatrix} x \\ vx \\ y \\ vy \end{bmatrix} \quad (25)$$

C. AUTONOMOUS PRECISION LANDING PLANNER

In order to achieve the landing task in a safe and precise manner, a landing planner is introduced. Once the landing task is triggered, the planner ensures the vehicle to follow a landing procedure (Figure 5) that consists of five phases:

Phase 1. Landing area approach

In this phase, the vehicle is driven to reach the landing area horizontally while maintaining its altitude.

Phase 2. Landing target approach

Once the LT is detected (by the IR camera), the planner will steer the quadcopter to approach the target horizontally until the horizontal distance between the vehicle and the target satisfies a given condition.

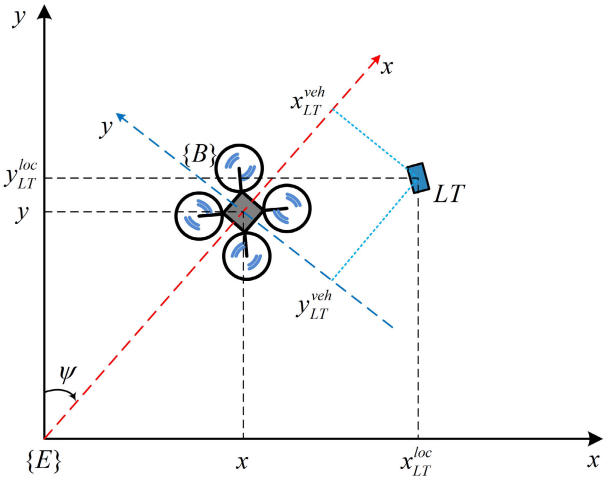

FIGURE 4. The landing target position in the vehicle-body-fixed frame ({*B*}) and in the local earth-fixed frame ({*E*}).

Phase 3. Descent over the landing target

When the quadcopter is horizontally close enough to the target, it starts descending while maintaining its horizontal distance to the target.

During Phase 2 and Phase 3, if the LT is not detected (in a certain duration), the planner will consider the target temporally lost and will manipulate the vehicle to climb to a predefined altitude (called search altitude) to search for the target.

Phase 4. Final approach

When the quadcopter is vertically close to the LT, the planner will operate the final approach phase, including decreasing the vehicle throttle (so that it can land quickly onto the landing platform) and disabling stabilized control.

Phase 5. Landing complete

Once the vehicle is stationary on the landing platform, the planner will disarm it, and the landing task is completed.

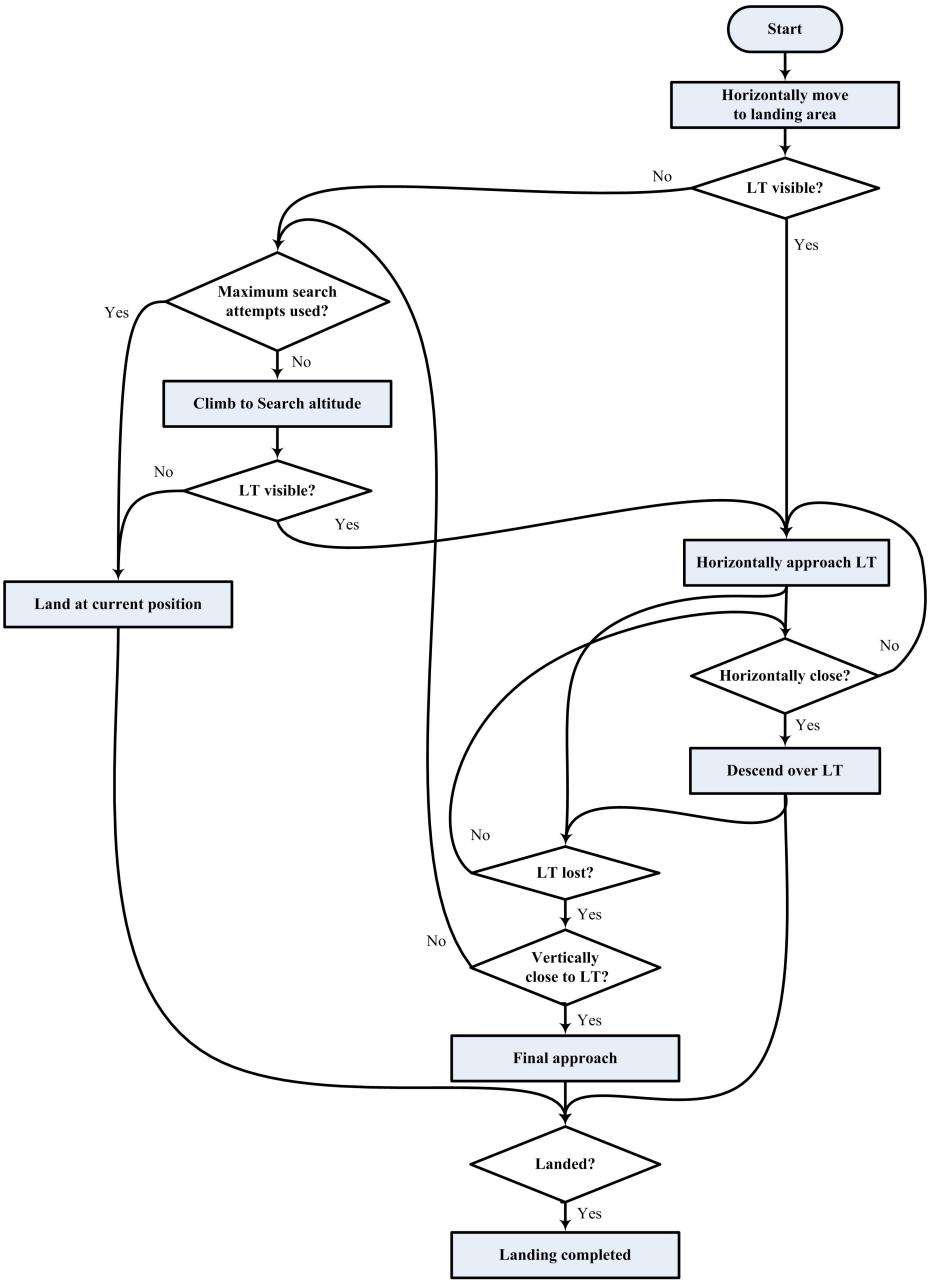

FIGURE 5. Block diagram of the autonomous landing procedure allowing the landing task to be achieved safely and precisely.

IV. EXPERIMENT AND DISCUSSIONS

A. EXPERIMENTAL SETUP

1) QUADCOPTER PLATFORM

We use a DJI-F450 quadcopter as the experimental platform (Figure 6) which is operated by an onboard flight computer unit (FCU) Pixhawk. The quadcopter attitude and acceleration are provided by an inertial navigation system (INS). We use a commercially available laser ranging sensor LidarLite V3 to measure the altitude and a commercial GPS receiver module to determine the position of the vehicle. Besides, a power supplying system (including a battery and a power adapter module), a set of remote control transmitter/receiver for the manual pilot, and a set of radio telemetry transmitter/receiver for ground station monitoring are used.

In order to determine the position of the LT precisely, we utilize an IR Pixy camera which is fast and easy to use. This camera can detect IR objects and provide information about x and y position of the center of the detected object in pixel. The data is updated at a frequency of 50 Hz through the UART interface. Additionally, an Odroid

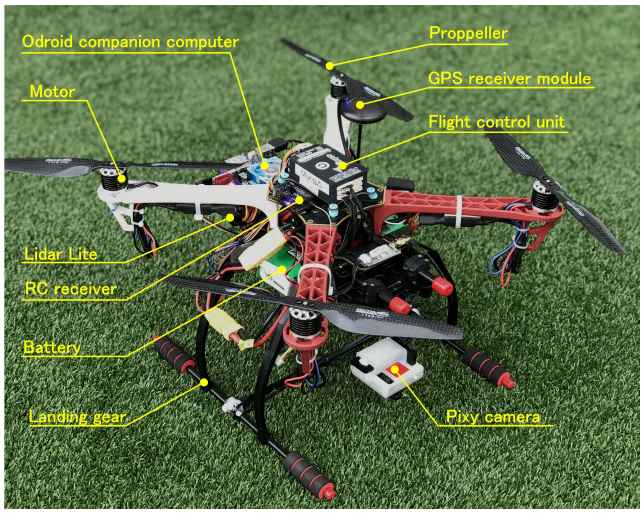

FIGURE 6. The experimental quadcopter platform with equipped avionics and mechanics devices.

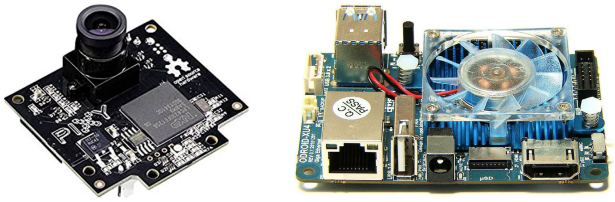

FIGURE 7. The IR Pixy camera and Odroid companion computer that are attached on the quadcopter.

TABLE 1. The parameters of the quadcopter dynamics and pixy camera.

Symbol	Value	Unit
m	2.7	kg
I_x	0.0173	kg.m^2
I_y	0.0141	kg.m^2
I_z	0.0223	kg.m^2
l	0.225	m
g	9.81	m/s^2
α_x	60	deg
α_y	47	deg

companion computer [40] is used for operating the proposed algorithm (including the robust altitude controller, the LTSE, and autonomous precision landing planner). This compact companion computer and the FCU communicate with each other through the Mavlink protocol. The parameters of the quadcopter dynamics and the Pixy camera are listed in Table 1.

2) HEAVING MOTION PLATFORM

The heaving motion platform is devised to simulate a UAV landing pad on a ship deck (Figure 8). The base of this platform is flat and thick, while the landing pad is a thinner and lighter wooden plate. The LT is an IR MarkOne beacon (see Figure 9) which is set at the center of the landing pad. Two

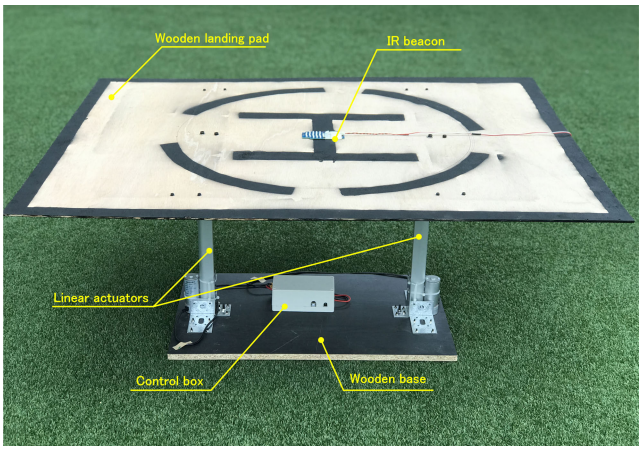

FIGURE 8. The heaving motion platform used to simulate a heaving ship deck.

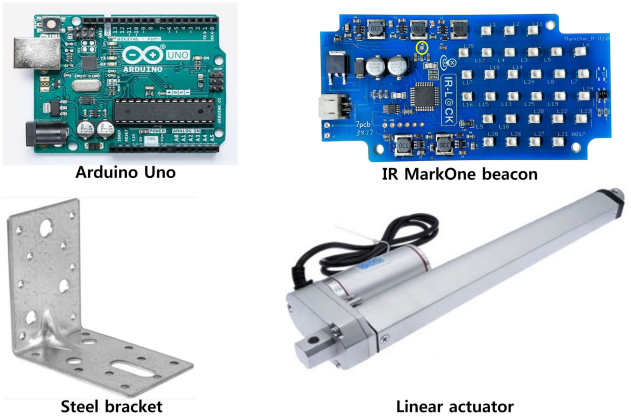

FIGURE 9. The devices used to make the heaving motion platform.

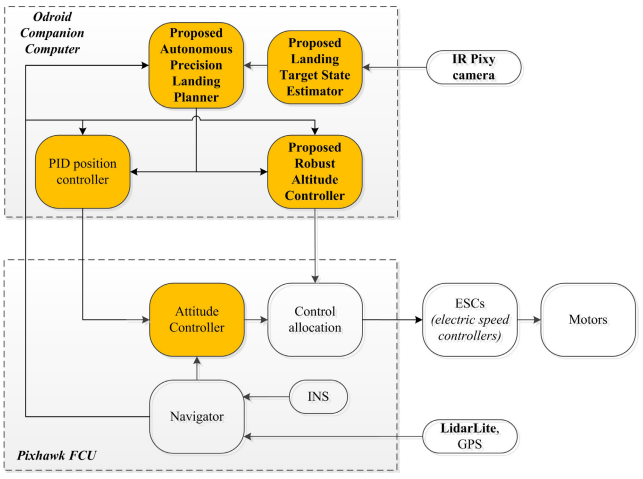

FIGURE 10. Block diagram of the system signal flow.

linear actuators are used to generate the heaving motion of the upper plate. These actuators are fixed to the wooden plates using steel brackets and are operated by a control box that consists of an Arduino Uno and motor drivers. When being

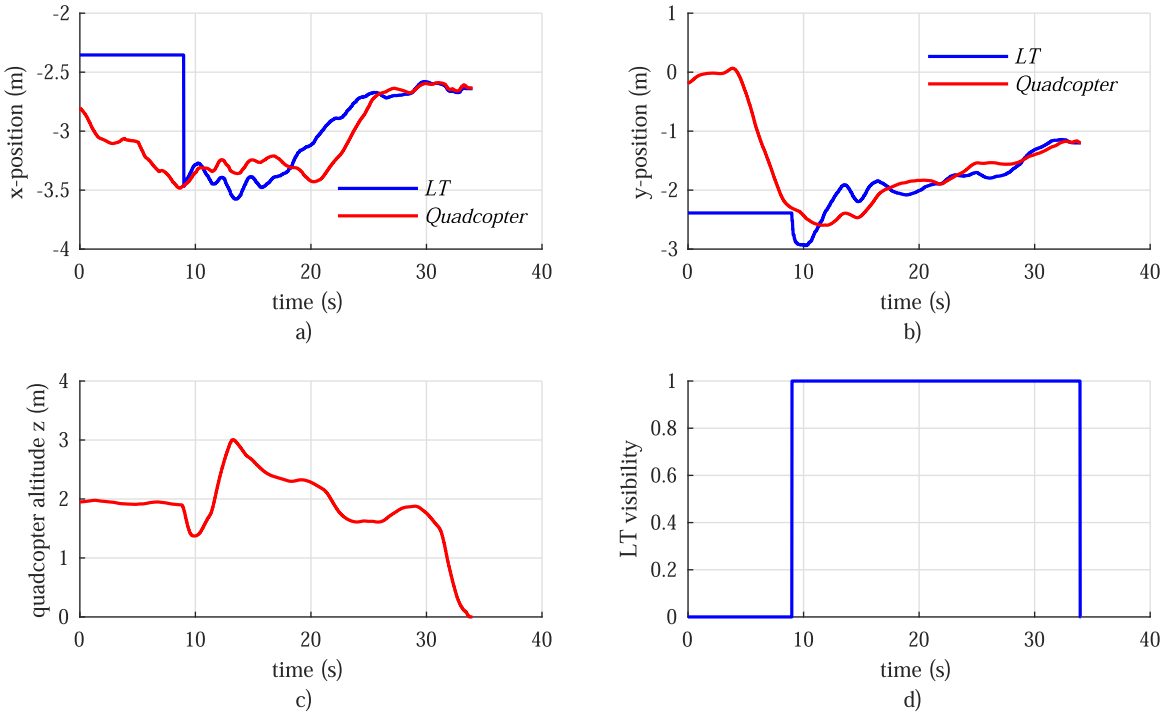

FIGURE 11. Landing target approaching control performance.

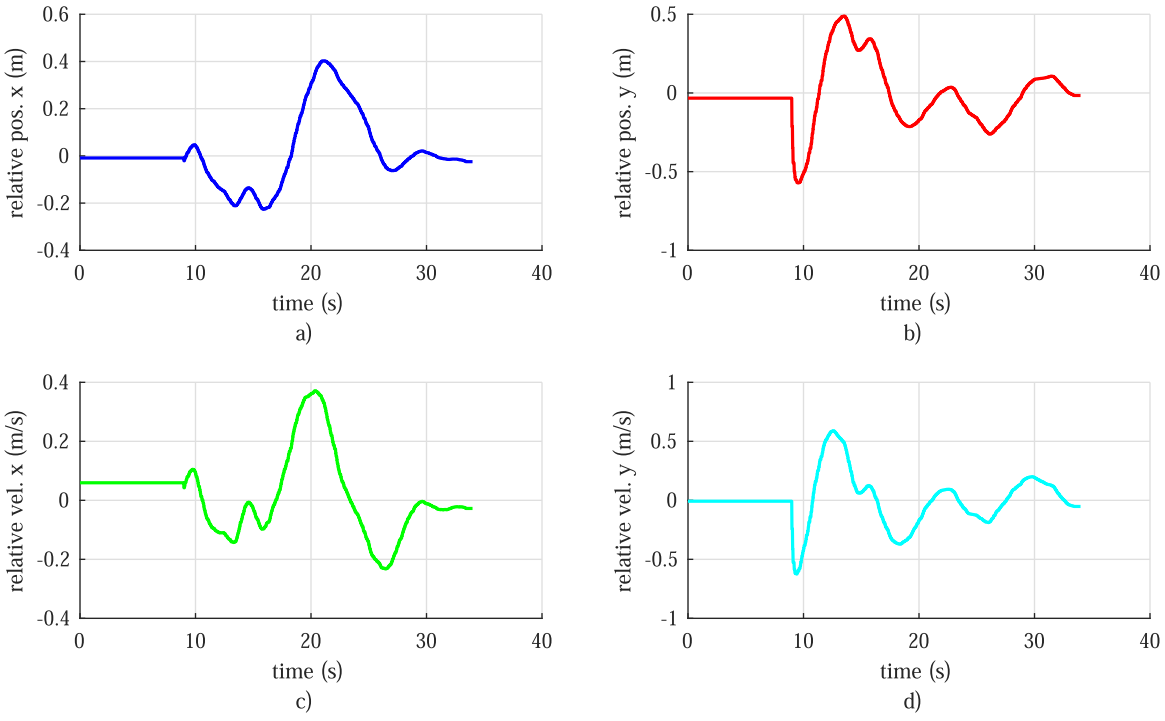

FIGURE 12. Landing target state estimation results.

supplied by a 12V-DC battery, this platform can generate a lift force up to 200 N with a heaving motion stroke of 300 mm and a speed of 90 mm/s. The detailed parameters of this platform are given in Table 2.

3) SOFTWARE

While the vehicle attitude controller is implemented on the Pixhawk FCU and runs at a frequency of 400 Hz, the proposed controller, LTSE, and landing planner are oper-

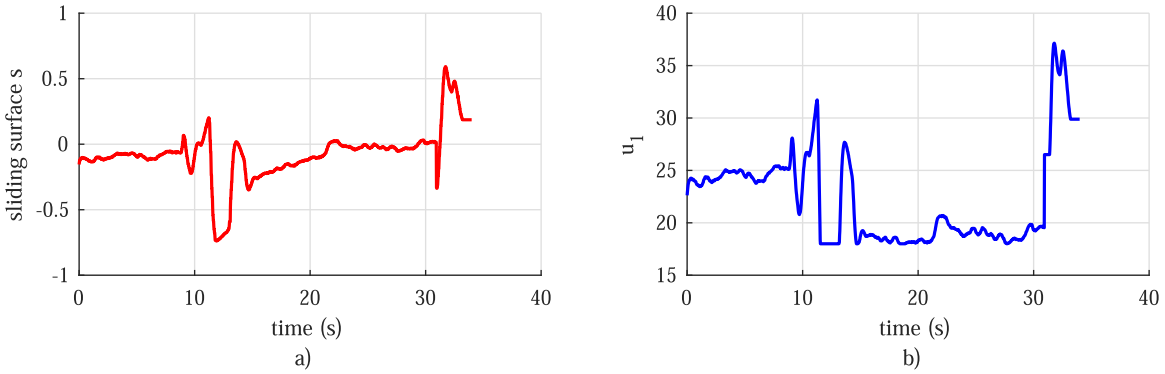

FIGURE 13. The sliding surface (s) and control input (u_1) performance of the proposed robust altitude controller.

TABLE 2. Parameters of the heaving motion platform.

Parameter	Valuet	Unit
Length	1.0	m
Width	0.8	m
Height	0.42 - 0.72	m
Heaving motion stroke	300	mm
Heaving motion speed	90	mm/s
IR beacon power supply	12	VDC
Actuator power supply	12	VDC
Controller box power supply	4.5 - 5.5	VDC

TABLE 3. Controller gains, observer gains, and camera data sampling time used in the experiment.

Symbol	Value and Unit	Description
k_1	0.82	Controller gain
k_2	8.9	Controller gain
λ	1.5	Observer gain
Δt	0.02 s	Pixy camera's data sampling time

ated by the Odroid companion computer at the same frequency of 100 Hz. The proposed altitude controller gains are listed in Table 3. It is worth noting that the horizontal position controller is designed using our multi-mode controller already presented in our previous work (see [33]), and the attitude controllers are designed using the PID control law. Since these controllers are beyond the scope of this paper, they will not be presented in this section. The system signal flows are briefly described by the block diagram in Figure 10.

B. EXPERIMENTAL RESULTS AND DISCUSSIONS

The experiment scenario is as follows: Firstly, the quadcopter takes-off and climbs to reach an altitude of 1.9 m above the test site floor (we chose this value after considering the fact that our test site is covered by nets with a 3.5 m maximum-height). Secondly, while the vehicle is hovering at a position far from the landing area (about 2.5 m away), the landing task is triggered. Since the landing area's position in the local frame is given, the quadcopter moves horizontally (altitude maintained) to that area based on the GPS signal. Afterward, the vehicle performs the IR-Pixy-camera-based precision landing procedure, as described in Figure 5. Videos of our experiments can be found at *https://youtu.be/3NljwomPZYw*.

The experimental results are presented in Figures 11 through 13. In order to focus on the landing task performance, the flight data is shown from the landing task starting time point. The vehicle's performance can be seen consisting of two stages: (i) GPS-based landing area approach; and (ii) IR-Pixy-camera-based precision landing.

The first stage covers the time period from $t = 0$ to $t = 9$ s (Figures 11a and 11b). During this stage, the quadcopter horizontally moves from its hovering position ($x = -2.7$ m and $y = -0.2$ m in the local frame) to the landing area ($x = -3.0$ m and $y = -2.0$ m in the local frame). While approaching the landing area, the quadcopter maintains its altitude of 1.9 m (Figure 11c), and the Pixy camera does not detect the LT (Figure 11d).

The second stage (from $t = 9$ s) starts when the vehicle has reached the landing area, and the camera detects the LT (Figure 11d). It can be seen in Figure 11c that, when the camera detects the landing platform, the vehicle's altitude decreases from 1.9 m to 1.5 m. The reason for this is because the landing platform, which is 0.42-0.72 m high, shortens the range measured by the ranging sensor when the vehicle is over the landing pad. Responding to the change of the measured range, from $t = 10$ s to $t = 28$ s, the altitude controller manipulates the quadcopter to climb up and down while the position controller is driving it to horizontally approach the IR beacon (Figures 11a and 11b). From $t = 28$ s, when the horizontal distance between the vehicle and the LT is less than the expected value, i.e., 0.15 m, the quadcopter starts to descend over the LT until the landing task is completed.

The landing target state estimation results (Figure 12) indicate the stability and reliability of the proposed LTSE. Besides, the stability and effectiveness of the proposed robust altitude controller are also verified as the sliding surface s is seen that varying in an appropriate range and converging to zero in a short time while the control input u_1 is stable and is free from the chattering phenomenon (Figure 13).

V. CONCLUSION

This paper presented a new method for a quadcopter landing precisely onto a heaving platform. The experimental results clearly demonstrate the effectiveness and reliability of the proposed method when showing that, by using our algorithm, the quadcopter completed its precision landing task. While our LTSE and the IR Pixy camera enable the quadcopter's ability to accurately determining and approaching the LT's position, the proposed robust altitude controller allows it to land stably and rapidly despite the influences of the ground effect and external disturbances. The autonomous landing procedure ensures that the precision landing task is achieved safely and reliably. The proposed method is scalable and applicable to real-world applications that require the vehicle to land onto heaving objects such as a ship deck. Our future work will be directed to designing and experiment with a landing algorithm to achieve a quadcopter precision landing onto a three-dimensional moving platform.

REFERENCES

[1] O. I. D. Bashi, W. Z. W. Hasan, N. Azis, S. Shafie, and H. Wagatsuma, "Unmanned aerial vehicle quadcopter: A review," *J. Comput. Theor. Nanoscience*, vol. 38, pp. 529–554, Dec. 2016.

[2] N. S. Ozbek, M. Onkol, and M. O. Efe, "Feedback control strategies for quadrotor-type aerial robots: A survey," *Trans. Inst. Meas. Control*, vol. 14, no. 5, pp. 5663–5675, 2017.

[3] N. Xuan-Mung and S. K. Hong, "Robust backstepping trajectory tracking control of a quadrotor with input saturation via extended state observer," *Appl. Sci.*, vol. 9, no. 23, p. 5184, Nov. 2019.

[4] P. E. I. Pounds, D. R. Bersak, and A. M. Dollar, "Stability of small-scale UAV helicopters and quadrotors with added payload mass under PID control," *Auto. Robots*, vol. 33, nos. 1–2, pp. 129–142, Aug. 2012.

[5] A. T. Nguyen, N. Xuan-Mung, and S.-K. Hong, "Quadcopter adaptive trajectory tracking control: A new approach via backstepping technique," *Appl. Sci.*, vol. 9, no. 18, p. 3873, Sep. 2019.

[6] H. Wang, Y. Pan, S. Li, and H. Yu, "Robust sliding mode control for robots driven by compliant actuators," *IEEE Trans. Control Syst. Technol.*, vol. 27, no. 3, pp. 1259–1266, May 2019.

[7] S. Ding and S. Li, "Second-order sliding mode controller design subject to mismatched term," *Automatica*, vol. 77, pp. 388–392, Mar. 2017.

[8] H. Wang, Q. Zhang, J. Xian, and I.-M. Chen, "Robust finite-time output feedback control for systems with unpredictable time-varying disturbances," *IEEE Access*, vol. 8, pp. 52268–52277, 2020.

[9] X.-H. Chang, Y. Liu, and M. Shen, "Resilient control design for lateral motion regulation of intelligent vehicle," *IEEE/ASME Trans. Mechatronics*, vol. 24, no. 6, pp. 2488–2497, Dec. 2019.

[10] H. W. Ho, G. C. H. E. de Croon, E. van Kampen, Q. P. Chu, and M. Mulder, "Adaptive gain control strategy for constant optical flow divergence landing," *IEEE Trans. Robot.*, vol. 34, no. 2, pp. 508–516, Apr. 2018.

[11] V. M. Goncalves, R. McLaughlin, and G. A. S. Pereira, "Precise landing of autonomous aerial vehicles using vector fields," *IEEE Robot. Autom. Lett.*, vol. 5, no. 3, pp. 4337–4377, Jul. 2020.

[12] D. Cabecinhas, R. Naldi, C. Silvestre, R. Cunha, and L. Marconi, "Robust landing and sliding maneuver hybrid controller for a quadrotor vehicle," *IEEE Trans. Control Syst. Technol.*, vol. 24, no. 2, pp. 400–412, Mar. 2016.

[13] J. A. Dougherty and T. Y. Lee, "Adaptive gain control strategy for constant optical flow divergence landing," *J. Guid., Control, Dyn.*, vol. 39, pp. 1407–1416, 2016.

[14] B. Hu, L. Lu, and S. Mishra, "A control architecture for time-optimal landing of a quadrotor onto a moving platform," *Asian J. Control*, vol. 20, no. 5, pp. 1701–1712, 2017.

[15] J. Ghommam and M. Saad, "Autonomous landing of a quadrotor on a moving platform," *IEEE Trans. Aerosp. Electron. Syst.*, vol. 53, no. 3, pp. 1504–1519, Jun. 2017.

[16] D. Tzoumanikas, W. Li, M. Grimm, K. Zhang, M. Kovac, and S. Leutenegger, "Fully autonomous micro air vehicle flight and landing on a moving target using visual-inertial estimation and model-predictive control," *J. Field Robot.*, vol. 36, no. 1, pp. 49–77, Jan. 2019.

[17] C. M. Huang, M. L. Chiang, and T. S. Hung, "Visual servoing of a micro quadrotor landing on a ground platform," *Int. J. Control, Autom. Syst.*, vol. 15, no. 6, pp. 2791–2805, 2017.

[18] A. Almeshal and M. Alenezi, "A vision-based neural network controller for the autonomous landing of a quadrotor on moving targets," *Robotics*, vol. 7, no. 4, p. 71, Nov. 2018.

[19] P. R. Palafox, M. Garzón, J. Valente, J. J. Roldán, and A. Barrientos, "Robust visual-aided autonomous takeoff, tracking, and landing of a small UAV on a moving landing platform for life-long operation," *Appl. Sci.*, vol. 9, no. 13, p. 2661, Jun. 2019.

[20] Y. Qi, J. Jiang, J. Wu, J. Wang, C. Wang, and J. Shan, "Autonomous landing solution of low-cost quadrotor on a moving platform," *Robot. Auto. Syst.*, vol. 119, pp. 64–76, Sep. 2019.

[21] P. Serra, R. Cunha, T. Hamel, D. Cabecinhas, and C. Silvestre, "Landing of a quadrotor on a moving target using dynamic image-based visual servo control," *IEEE Trans. Robot.*, vol. 32, no. 6, pp. 1524–1535, Dec. 2016.

[22] A. Borowczyk, D. T. Nguyen, A. P. V. Nguyen, D. Q. Nguyen, D. Saussie, and J. L. Ny, "Autonomous landing of a multirotor micro air vehicle on a high velocity ground vehicle," *IFAC-PapersOnLine*, vol. 50, pp. 10488–10494, Jan. 2017.

[23] X. Liu, S. Zhang, J. Tian, and L. Liu, "An onboard vision-based system for autonomous landing of a low-cost quadrotor on a novel landing pad," *Sensors*, vol. 19, no. 21, p. 4703, Oct. 2019.

[24] O. Araar, N. Aouf, and I. Vitanov, "Vision based autonomous landing of multirotor UAV on moving platform," *J. Intell. Robot. Syst.*, vol. 85, no. 2, pp. 369–384, 2017.

[25] C. K. Tan, J. Wang, Y. C. Paw, and F. Liao, "Robust linear output feedback controller for autonomous landing of a quadrotor on a ship deck," *Int. J. Control*, vol. 15, pp. 2810–2818, 2019.

[26] L. Tan, J. Wu, X. Yang, and S. Song, "Research on optimal landing trajectory planning method between an UAV and a moving vessel," *Appl. Sci.*, vol. 9, no. 18, p. 3708, Sep. 2019.

[27] Q. Lu, B. Ren, and S. Parameswaran, "Shipboard landing control enabled by an uncertainty and disturbance estimator," *J. Guid., Control, Dyn.*, vol. 41, no. 7, pp. 1502–1520, Jul. 2018.

[28] Y. Huang, Z. Zheng, L. Sun, and M. Zhu, "Saturated adaptive sliding mode control for autonomous vessel landing of a quadrotor," *IET Control Theory Appl.*, vol. 12, no. 13, pp. 1830–1842, Sep. 2018.

[29] L. Wang and X. Bai, "Quadrotor autonomous approaching and landing on a vessel deck," *J. Intell. Robot. Syst.*, vol. 9, pp. 1830–1842, Dec. 2017.

[30] C. K. Tan, J. Wang, Y. C. Paw, and F. Liao, "Autonomous ship deck landing of a quadrotor using invariant ellipsoid method," *IEEE Trans. Aerosp. Electron. Syst.*, vol. 52, no. 2, pp. 891–903, Apr. 2016.

[31] L. Danjun, Z. Yan, S. Zongying, and L. Geng, "Autonomous landing of quadrotor based on ground effect modelling," in *Proc. 34th Chin. Control Conf. (CCC)*, Hangzhou, China, Jul. 2015, pp. 5647–5652.

[32] X. Kan, J. Thomas, H. Teng, H. G. Tanner, V. Kumar, and K. Karydis, "Analysis of ground effect for small-scale UAVs in forward flight," *IEEE Robot. Autom. Lett.*, vol. 4, no. 4, pp. 3860–3867, Oct. 2019.

[33] N. Xuan-Mung and S.-K. Hong, "Improved altitude control algorithm for quadcopter unmanned aerial vehicles," *Appl. Sci.*, vol. 9, no. 10, p. 2122, May 2019.

[34] N. Xuan-Mung and S.-K. Hong, "Barometric altitude measurement fault diagnosis for the improvement of quadcopter altitude control," in *Proc. 19th Int. Conf. Control, Autom. Syst. (ICCAS)*, Jeju, South Korea, Oct. 2019, pp. 1359–1364.

[35] W. H. Chen, J. Yang, L. Gou, and S. Li, "Disturbance-observer-based control and related methods—An overview," *IEEE Trans. Ind. Electron.*, vol. 63, no. 2, pp. 1083–1095, Sep. 2016.

[36] H. K. Khalil, *Nonlinear Systems*, 3rd ed. Upper Saddle River, NJ, USA: Prentice-Hall, 2002.

[37] P. Kim, *Kalman Filter for Beginners With MATLAB Examples*. Jeonju-si, South Korea: A-JIN Publishing Company, 2010.

[38] (2020). *CMUcam5 Pixy*. [Online]. Available: http://www.cmucam.org/projects/cmucam5

[39] (2020). *Flame Wheel ARF Kit*. [Online]. Available: https://www.dji.com/kr/flame-wheel-arf/spec

[40] (2020). *Odroid XU4 User Manual*. [Online]. Available: https://magazine.odroid.com/wp-content/uploads/odroid-xu4-user-manual.pdf

NGUYEN XUAN-MUNG (Member, IEEE) received the B.S. degree in mechatronics from the Hanoi University of Science and Technology, Hanoi, Vietnam, in 2014, and the M.S. degree in aerospace engineering from Sejong University, Seoul, South Korea, in 2017, where he is currently pursuing the Ph.D. degree. From 2014 to 2015, he was with Samsung Electronics Vietnam Company Ltd., Vietnam. His research interests include unmanned aerial vehicles, nonlinear control systems, mechatronics, and robotics.

SUNG KYUNG HONG received the B.S. and M.S. degrees in mechanical engineering from Yonsei University, Seoul, South Korea, in 1987 and 1989, respectively, and the Ph.D. degree from Texas A&M University, College Station, TX, USA, in 1998. From 1989 to 2000, he was with the Flight Dynamics and Control Laboratory and the Unmanned Aerial Vehicle System Division, Agency for Defense Development, South Korea. He is currently a Full Professor with the Department of Aerospace Engineering, Sejong University, South Korea. His research interests include fuzzy logic controls, inertial sensor applications, and flight control systems.

NGOC PHI NGUYEN received the B.S. degree in mechatronics engineering from the HCMC University of Technology and Education, in 2010, the M.S. degree in mechatronics engineering from Vietnamese-German University, Vietnam, in 2015, and the Ph.D. degree in aerospace engineering from Sejong University, Seoul, South Korea, in 2020. He is currently an Assistant Professor with the Department of Aerospace Engineering, Sejong University. His research interests include fault-tolerant control, nonlinear control, intelligent control, and formation control.

LE NHU NGOC THANH HA received the B.S. degree in mechanical engineering from the HCMC University of Technology and Education, in 2011, the M.S. degree in mechanical engineering from the HCMC University of Technology, Vietnam, in 2015, and the Ph.D. degree from the Faculty of Mechanical and Aerospace Engineering, Sejong University, Seoul, South Korea, in 2019. He is currently an Assistant Professor with the Faculty of Intelligent Mechatronics Engineering, Sejong University. His research interests include nonlinear control, mechatronics, and robotics. He received an Outstanding Research Award in Sejong University, in 2019. He also serves as a Guest Editor of *Sensor* journal (MDPI) and *Applied Sciences* journal (MDPI).

TIEN-LOC LE (Member, IEEE) was born in Vietnam, in 1985. He received the B.S. degree in electronics and telecommunication engineering from Lac Hong University, Vietnam, in 2009, the M.S. degree in electrical engineering from the Ho Chi Minh City University of Technology and Education, Vietnam, in 2012, and the Ph.D. degree in electrical engineering from Yuan Ze University, Taoyuan, Taiwan, in January 2018. From February 2018 to December 2018, he was a Postdoctoral Research Fellow with the Department of Electrical Engineering, Yuan Ze University. He is currently a Postdoctoral Research Fellow with the Faculty of Mechanical and Aerospace Engineering, Sejong University, Seoul, South Korea. He is also a Lecturer with the Faculty of Mechatronics and Electronics, Lac Hong University. His research interests include intelligent control systems, fuzzy neural networks, type-2 fuzzy neural networks, and cerebellar model articulation controllers.